NJC

Accepted Manuscript

This is an *Accepted Manuscript*, which has been through the Royal Society of Chemistry peer review process and has been accepted for publication.

Accepted Manuscripts are published online shortly after acceptance, before technical editing, formatting and proof reading. Using this free service, authors can make their results available to the community, in citable form, before we publish the edited article. We will replace this *Accepted Manuscript* with the edited and formatted *Advance Article* as soon as it is available.

You can find more information about *Accepted Manuscripts* in the Information for Authors.

Please note that technical editing may introduce minor changes to the text and/or graphics, which may alter content. The journal's standard Terms & Conditions and the Ethical guidelines still apply. In no event shall the Royal Society of Chemistry be held responsible for any errors or omissions in this *Accepted Manuscript* or any consequences arising from the use of any information it contains.

ROYAL SOCIETY OF CHEMISTRY

www.rsc.org/njc

NJC

RSCPublishing

LETTER

Targeted delivery of photoactive diazido Pt^{IV} complexes conjugated with fluorescent carbon dots

Cite this: DOI: 10.1039/x0xx00000x

Xiao-Dong Yang,[a‡] Hui-Jing Xiang,[a‡] Lu An,[b] Shi-Ping Yang,[b] and Jin-Gang Liu*[a]

Received 00th xxxx 2014,
Accepted 00th xxxx 2014

DOI: 10.1039/x0xx00000x

www.rsc.org/

A novel Pt^{IV}-azide@carbon dots (CDs) nanoplatform for photo-controlled targeted platinum drug delivery was developed. The Pt^{IV}-N_3-FA@CDs nanoplatform selectively targeted folate-receptor overexpressed cancer cells while being simultaneously traced based on its inherent fluorescence; and it showed no dark cytotoxicity even in the presence of reducing glutathione, whereas it was readily photo-activated by either UV or visible light, producing cytotoxicity at a level comparable with that of cisplatin.

Platinum (Pt) complexes, including cisplatin, carboplatin, and oxaliplatin have been successfully applied in clinics as chemotherapeutic reagents for the treatment of various solid tumors and cancers. Severe toxic side effects and drug resistance, however, have restricted their efficacy. The use of a relatively inert Pt^{IV} prodrug together with a nanocarrier is a promising approach to improve the efficacy of Pt-based anticancer complexes. The Pt^{IV} prodrug is usually activated to a reactive Pt^{II} drug in acidic tumor cells through reduction by intracellular reducing agents such as glutathione (GSH), cysteine, and metallothionein.[1-3] Nevertheless, premature reduction in the bloodstream also produces a reactive Pt^{II} drug that may lead to detrimental side effects. Over the past decades, numerous new Pt complexes and their decorated nano-delivery systems have been intensively explored.[1-24] Among these, nonclassical Pt^{IV}-azide complexes are considered to be a unique candidate because of their chemical inertness and photoactivable properties. The Pt^{IV}-azide complexes do not react with the intracellular biomolecules in the dark, such as guanosine 5′-monophosphate (5′-GMP) and the reducing agent GSH. On the other hand, these can be readily activated by light (e.g., UV, blue, or green light), converting the Pt^{IV} prodrug to Pt^{II}. The *in situ*-generated Pt^{II} drug can then kill cancer cells by a mechanism distinct from that of cisplatin.[4-12] Recently, several nano-delivery systems consisting of photoactivable Pt^{IV} azide prodrugs with micellar nanoparticles[11] or upconversion nanoparticles[9, 12] have been reported, where the reactive Pt^{II} component was released upon light illumination. However, till date, there are no reports on the targeted delivery of Pt^{IV} azide prodrugs to cancer cell lines.

Targeted delivery of a photoactivable Pt^{IV} prodrug using light is a potential approach for minimizing the defects of Pt-based chemotherapy. Photoactivation can be targeted to a spatially directed site, thereby avoiding damage to adjacent normal tissues.[13-17]

Carbon dots (CDs) have emerged as a new class of drug carriers. It has some unique properties, such as excitation-dependent multicolor emission, water solubility, good biocompatibility, cell permeability, and non-blinking photo-stability.[25-31] Due to its inherent fluorescence, CDs allow for real-time monitoring the trace of the drug delivery system in cellular microenvironment. In addition, CDs are much safer for biological applications compared with metal containing quantum dots and nanoparticles.

We report herein a novel Pt^{IV}-N_3-FA@CDs nanoplatform that combined the excellent characteristics of CDs and the unique properties of Pt^{IV} azide complexes for photo-controlled targeted platinum drug delivery. This newly developed Pt^{IV}-N_3-FA@CDs nanoplatform is capable of targeted delivery of the Pt^{IV} prodrug to specific cancer cell lines while being fluorescent traced, with subsequent visible light activation to induce cell cytotoxicity comparable with that of cisplatin. This represents the first example of Pt^{IV} azide nanodelivery system showing target directing and fluorescence tracing at the same time.

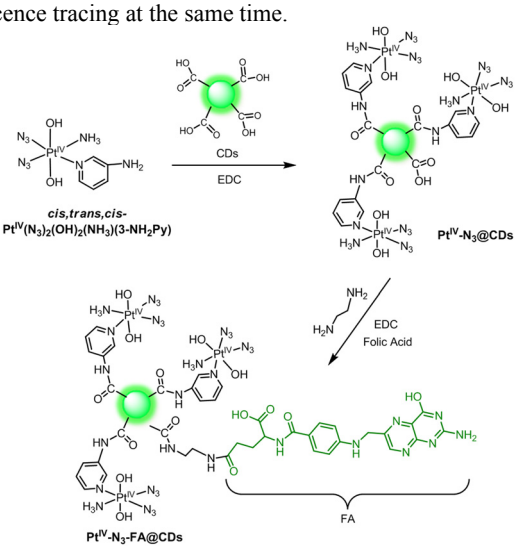

Scheme 1 Synthesis of the Pt^{IV}-N_3-FA@CDs nanoplatform.

The multifunctional Pt^{IV}-N_3-FA@CDs nanoplatform is composed of a photoactive Pt^{IV} azide prodrug, and folic acid (FA) molecules covalently incorporated on the CDs surface, where the Pt^{IV}-azide compound, *cis*, *trans*, *cis*-$Pt^{IV}(N_3)_2(OH)_2(NH_3)(3\text{-}NH_2Py)$, was conjugated to the CDs through the nonleaving group 3-aminopyridine ligand (Scheme 1). CDs not only act as prodrug carriers but also as cell imaging agents, which can aid in tracing the location of the nanoplatform at the subcellular level. FA was attached to the CD surface as a targeting group on the basis of its high affinity to the folate receptor (FR), which is often overexpressed in a wide range of human cancerous cells.[32]

CDs were prepared from activated carbon by refluxing in oxidative acid condition and purifying by dialysis.[33] The Pt^{IV}-azide was then covalently incorporated on the surface of CDs through the formation of an amide bond between the aminopyridine group from the Pt^{IV} azide prodrug and the carboxyl group from CDs, which in turn generated the precursor Pt^{IV}-N_3@CDs. The surplus carboxyl groups on CDs were further treated with an excess amount of ethylenediamine and then reacted with FA to produce the final nanoplatform Pt^{IV}-N_3-FA@CDs (Scheme 1, the detailed procedure is described in ESI).

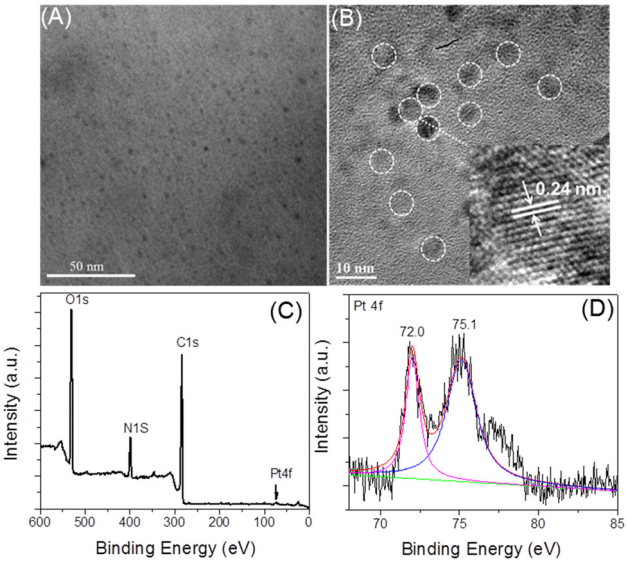

Fig. 1 (A) TEM image of Pt^{IV}-N_3-FA@CDs. (B) HRTEM image of Pt^{IV}-N_3-FA@CDs. (C) XPS survey spectrum of Pt^{IV}-N_3-FA@CDs. (D) High-resolution Pt 4f XPS spectrum of Pt^{IV}-N_3-FA@CDs.

The morphology of Pt^{IV}-N_3-FA@CDs was analyzed using a transmission electron microscope (TEM). Fig. 1A shows a TEM image of Pt^{IV}-N_3-FA@CDs, which is a globular-shaped particle with an average size of approximately 5 nm. Well-resolved lattice fringes were observed on high-resolution TEM images, with a *d*-spacing value of 0.24 nm (Fig. 1B), indicating the graphitic nature of CDs.[25] The composition of Pt^{IV}-N_3-FA@CDs was analyzed by X-ray photoelectron spectroscopy (XPS). The XPS survey spectrum of Pt^{IV}-N_3-FA@CDs showed that it was composed of C, N, O, and Pt (Fig. 1C). The high-resolution XPS spectrum of Pt 4f displayed two peaks at 75.1 eV and 72.0 eV (Fig. 1D), which were assigned to the binding energy value of Pt $4f_{5/2}$ and Pt $4f_{7/2}$, respectively.[29, 30] The Pt content of Pt^{IV}-N_3-FA@CDs was determined to be 2.1 wt% by atomic absorption spectroscopy. The zeta potential measurement of Pt^{IV}-N_3-FA@CDs revealed a surface potential of −0.05 mV, suggesting its almost neutral characteristic surface (Fig. S2).

The FTIR spectra of Pt^{IV}-N_3-FA@CDs displayed a peak at 2056 cm^{-1} (Fig. 2A), which were assigned to the stretching vibration of the azido ligand. This peak showed a 15-wavenumber upshift relative to the ungrafted Pt^{IV} azide complex (ν_{N3} = 2041 cm^{-1}). The IR spectrum of bare CDs revealed characteristic carboxylic acid vibrations, where a very strong band at 1724 cm^{-1} was ascribed to the stretching vibration ($\nu_{C=O}$) of the carboxyl groups in CDs. This peak shifted to 1605 cm^{-1} after the Pt^{IV} azide complex was covalently grafted on CDs (Fig. 2A), indicating the formation of an amide bond. There was a shoulder at approximately 1724 cm^{-1} in the IR spectrum of the precursor Pt^{IV}-N_3@CDs (Fig. 2A). This indicated the presence of unreacted remaining carboxylic groups in CDs that were further activated to react with FA, thus resulting in the formation of the Pt^{IV}-N_3-FA@CDs nanoplatform. The broad absorption bands at 3000–3500 cm^{-1} were assigned to the stretching vibrations of O-H (ν_{OH}) and N-H (ν_{NH}) in Pt^{IV}-N_3-FA@CDs. The UV-vis absorption spectrum of Pt^{IV}-N_3-FA@CDs was dominated by the absorption of CDs, where a broad yet weak absorption band at approximately 275 nm was detected. This band was approximately equal to the electronic absorption band of FA (λ_{max}: 280 nm), which indicated the successful anchoring of FA to the nanoplatform (Fig. 2B). The Pt^{IV}-N_3-FA@CDs showed a fluorescence emission peak centered at approximately 450 nm when excited at 360 nm. The fluorescence intensity increased, whereas the emission peak revealed a blue shift of approximately 50 nm compared with that of the as-prepared CDs (E_m: approximately 500 nm; Fig. S4).

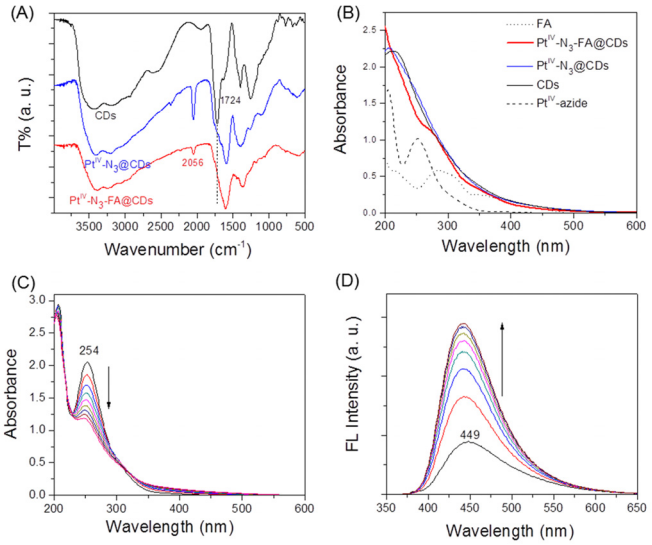

Fig. 2 (A) FTIR spectra of CDs (black line), Pt^{IV}-N_3@CDs (blue line), and Pt^{IV}-N_3-FA@CDs (red line). (B) UV-vis spectra of the Pt^{IV}–azide compound (black dotted line), CDs (black solid line), Pt^{IV}-N_3@CDs (blue solid line), and Pt^{IV}-N_3-FA@CDs (red solid line) in aqueous solution. (C) UV-vis spectra of the Pt^{IV}–azide compound under UV light irradiation (3.3 mW/cm^2). Recording interval: 10 min. (D) Fluorescence spectra of Pt^{IV}-N_3-FA@CDs under UV light irradiation (3.3 mW/cm^2). Recording interval: 10 min.

Premature reduction of the Pt^{IV} prodrug in the bloodstream before reaching a tumor cell produces reactive Pt^{II} that could lead to severe side effects. Electrochemical studies on the Pt^{IV}–azide compound have revealed a reduction potential of −0.59 V *vs.* NHE in PBS solution (pH 7.0; Fig. S5), which was more negative than that of the clinically used satraplatin (−0.053 V *vs.* NHE).[22, 34] When GSH was added to the Pt^{IV}–azide solution, no UV-vis spectral change was detected, suggesting that GSH did not reduce the Pt^{IV}–azide compound. On the other hand, the Pt^{IV}–azide compound was readily

reduced by light. Under UV light irradiation (3.3 mW/cm^2), the UV-vis spectra of the Pt^{IV}–azide compound demonstrated a significant decrease in the $N_3^- \rightarrow Pt$ LMCT band at 254 nm,[10] suggesting the photoreduction of Pt^{IV} to Pt^{II} (Fig. 2C). The feasibility of the photoactivation of the Pt^{IV}-N_3-FA@CDs nanoplatform was then investigated. Given that the UV-vis spectrum of Pt^{IV}-N_3-FA@CDs was dominated by the absorption of CDs, UV-vis spectroscopy was determined to be an inappropriate approach in monitoring the photoactivation process. However, this process could be detected through changes in the intensity of the nanoplatform fluorescence. After activation by UV light (3.3 mW/cm^2), the fluorescence intensity of Pt^{IV}-N_3-FA@CDs in aqueous solution dramatically increased (Fig. 2D), suggesting the formation of a product with enhanced fluorescence intensity. This observation could be attributable to the photoreduction of Pt^{IV} to Pt^{II} by the photoelectrons derived from both the azido ligand and the excited CDs. Photo-induced electron transfer from exited CDs to the substrate has also been observed in other systems.[25, 26, 35, 36] As a control, the fluorescence spectra of the bare CDs showed no spectral change after light irradiation (Fig. S6). The Pt^{IV}-N_3-FA@CDs nanoplatform could also be activated by visible light (Fig. S6).

We employed FR-positive [FR(+)] human cervical HeLa cells for FR-mediated targeting and FR-negative [FR(−)] human breast MCF-7 tumor cells as controls. HeLa cells are known to overexpress FRs outside its membrane, whereas MCF-7 cells express very low levels of FR.[37] The selective binding of the Pt^{IV}-N_3-FA@CDs nanoplatform to the targeted HeLa cells was determined by confocal laser scanning microscopy. Confocal images of the internalized Pt^{IV}-N_3-FA@CDs within cells were obtained after incubation with the cancer cell lines. The internalization of Pt^{IV}-N_3-FA@CDs in cells was readily recognized by its inherent fluorescence. Fig. 3 clearly shows the selective accumulation of Pt^{IV}-N_3-FA@CDs in the FR(+) HeLa cells, whereas its uptake in the FR(−) MCF-7 cells was much lower. It was found that the nanoplatform localized to both the cytosol and nuclei of HeLa cells.

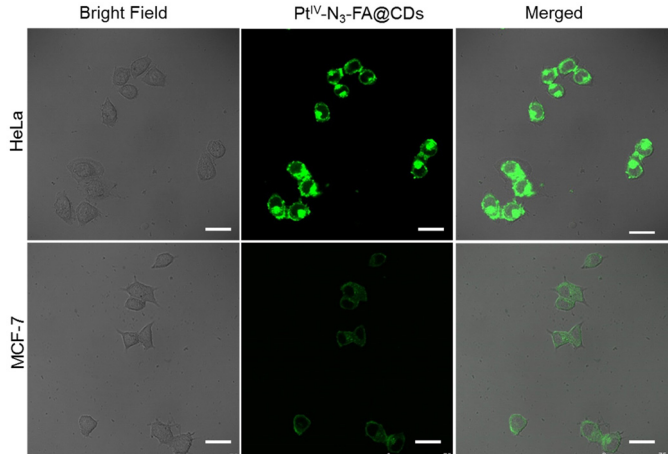

Fig. 3 Confocal microscopy images of FR (+) HeLa and FR (−) MCF-7 cells treated with 100 μg/mL of the nanoplatform for 6 h at 37 °C. The images were obtained using an excitation wavelength of 488 nm and recording the corresponding fluorescence in the range of 500–550 nm. Scale bar: 30 μm.

The cytotoxic effects of the Pt^{IV}-N_3-FA@CDs nanoplatform were investigated at various concentrations by MTT (3-(4,5-dimethylthiazol-2-yl)-2,5-diphenyltetrazolium bromide) assay. Under dark conditions, the nanoplatform did not have any cytotoxic effects against all the tested concentrations (0–400 μg/mL) (Fig. 4). On the other hand, in the presence of visible light irradiation (>400 nm, 180 mW/cm^2, 20 min), the viability of HeLa cells significantly decreased (Fig. 4). The cell death did not result from the illumination of visible light itself, as in the control experiment without nanoplatform visible light illumination did not lead to cell lethality (concentration = 0, Fig.4). Accordingly, it was reasonable to suppose that the cell lethality stems from the photo-activated Pt active species, Pt^{II}. The half maximal inhibitory concentration (IC_{50}) of the Pt^{IV}-N_3-FA@CDs nanoplatform in HeLa cells was approximately 50 μg/mL, which corresponded to a Pt content of 1.0 μg/mL. This IC_{50} value was comparable with that of cisplatin under similar experimental conditions (Fig. S7). The mechanism associated with the cytotoxicity of Pt^{IV}-N_3-FA@CDs was elucidated by flow cytometry using the annexin V/PI assay. The proportion of live, dead, and apoptotic cells indicated that cell death caused by the nanoplatform after visible light activation was mainly through early apoptosis (Fig. S8).

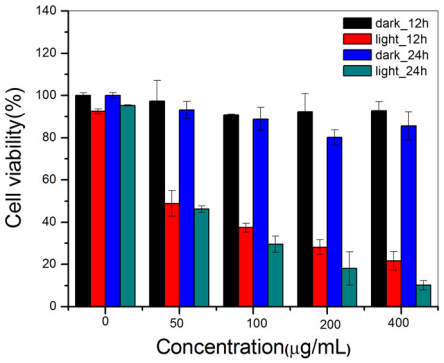

Fig. 4 Dark- and photo-induced lethality of HeLa cells treated with the Pt^{IV}-N_3-FA@CDs nanoplatform (concentration ranging from 0 to 400 μg/mL) for incubation of 12 h and 24 h, respectively. Irradiation with visible light (>400 nm, 180 mW/cm^{-2}, 20 min).

In summary, a Pt^{IV}-azide compound, *cis*, *trans*, *cis*-$Pt^{IV}(N_3)_2(OH)_2(NH_3)(3\text{-}NH_2Py)$, has been covalently loaded on the surface of fluorescent carbon dots whose surfaces were further functionalized by FA molecules.[38] This novel Pt^{IV}-N_3-FA@CDs nanoplatform selectively targeted FR-overexpressed cancer cells while being simultaneously traced based on its inherent fluorescence. In the dark, this Pt^{IV} prodrug was stable and intact even in the presence of reducing GSH; nevertheless, it was readily photo-activated and induced cytotoxicity at a level comparable with that of cisplatin. This Pt^{IV}-N_3-FA@CDs nanoplatform offers an alternative approach of tracing a specific therapy using a totally photo-controlled Pt-based theranostic agent.

Experimental Section

Confocal laser scanning microscopy

HeLa and MCF-7 cells were seeded on a plastic-bottomed μ-dish of diameter 35 mm, with a density of 10^4 cells and maintained at 37 °C in 5% CO_2 atmosphere for 24 h. The cells were then treated with the Pt^{IV}-N_3-FA@CDs solution (100 μg/mL) for 6 h. After incubation, the cells were washed twice with PBS and subjected to confocal fluorescence microscopy analysis.

MTT assay

The cells were seeded on a 96-well plate with a density of 5×10^4 cells per well and incubated in a humidified 5% CO_2 atmosphere for 24 h. The cell culture medium were removed and washed with PBS. Following that, different concentrations of Pt^{IV}-N_3-FA@CDs nanoplatform (0, 50, 100, 200, 400 μg/mL) in cell culture medium were added and incubated further for a period of 12 or 24 h at 37 °C in a humidified 5% CO_2 atmosphere. MTT (20 μL, 5.0 mg/mL) solution was added to each well. After 4 h of incubation at 37 °C, the cell culture medium was removed and the formazan crystals were lysed with 150 μL of DMSO. The absorbance was then measured at 490 nm using a microplate reader (Multiskan MK3, USA).

Visible light irradiation experiments: After incubation of the cells with different concentrations of the Pt^{IV}-N_3-FA@CDs nanoplatform (0, 50, 100, 200, 400 μg/mL) for 6 h, light irradiation was applied (λ > 400nm, 200 mW/cm^2, 20 min), and the cells were incubated for another 12 or 24 h.

Control experiment with cisplatin: After incubation of the cells with different concentrations of cisplatin (0, 2, 4, 5, 10 μM) for 6 h, light irradiation was applied (λ > 400nm, 200 mW/cm^2, 20 min), and the cells were incubated for another 24 h.

Acknowledgements

This study was financially supported by the NSF of China (21271072), the Program for Professor of Special Appointment (Eastern Scholar) at the Shanghai Institutions of Higher Learning, and sponsored by the Shanghai Pujiang Program (13PJ1401900).

Notes and references

[a] *Key Laboratory for Advanced Materials of MOE & Department of Chemistry, East China University of Science and Technology, Shanghai, 200237, P. R. China,* E-mail: liujingang@ecust.edu.cn
[b] *Key Laboratory of Resource Chemistry of MOE & Shanghai Key Laboratory of Rare Earth Functional Materials, Shanghai Normal University, Shanghai, 200234, P. R. China*.
‡ These authors contributed equally.
† Electronic Supplementary Information (ESI) available: Experimental details and additional figures. See DOI: 10.1039/b000000x/

1. E. Wong and C. M. Giandomenico, *Chem. Rev*., 1999, **99**, 2451.
2. L. Kelland, *Nat. Rev. Cancer*, 2007, **7**, 573.
3. A. V. Klein and T. W. Hambley, *Chem. Rev.* 2009, **109**, 4911.
4. P. J. Bednarski, F. S. Mackay and P. J. Sadler, *Anticancer Agents Med. Chem.* 2007, **7**, 75.
5. F. S. Mackay, J. A. Woods, P. Heringova, J. Kasparkova, A. M. Pizarro, S. A. Moggach, S. Parsons, V. Brabec and P. J. Sadler, *Proc. Natl. Acad. Sci.USA,* 2007, **104**, 20743.
6. N. J. Farrer, J. A. Woods, L. Salassa, Y. Zhao, K. S. Robinson, G. Clarkson, F. S. Mackay and P. J. Sadler, *Angew. Chem. Int. Ed*., 2010, **49**, 8905.
7. N. J. Farrer, J. A. Woods, V. P. Munk, F. S. Mackay and P. J. Sadler, *Chem. Res. Toxicol*., 2010, **23**, 413.
8. J. S. Butler; J. A. Woods; N. J. Farrer; M. E. Newton and P. J. Sadler, *J. Am. Chem. Soc*., 2012, **134**, 16508.
9. Y. Min, J. Li, F. Liu, E. K. L. Yeow and B. Xing, *Angew. Chem. Int. Ed.,* 2014, **53**, 1012.
10. A. Y. Sokolov and H. F. Schaefer III, *Dalton Trans.* 2011, **40**, 7571.
11. H. Xiao, G. T. Noble, J. F. Stefanick, R. Qi, T. Kiziltepe, X. Jing and B. Bilgicer, *J. Control. Release* 2014, **173**, 11.
12. Y. Dai, H. Xiao, J. Liu, Q. Yuan, P. Ma, D. Yang, C. Li, Z. Cheng, Z. Hou, P. Yang and J. Lin, *J. Am. Chem. Soc*., 2013, **135**, 18920.
13. J. S. Butler, P. J. Sadler, *Curr. Opin. Chem. Biol.*, 2013, **17**, 175.
14. R. A. Petros, J. M. Desimone, *Nat. Rev. Drug Discov*., 2010, **9**, 615.
15. X. Wang and Z. Guo, *Chem. Soc. Rev.* 2013, **42**, 202.
16. J. Wang, X. Wang, Y. Song, C. Zhu, J. Wang, K. Wang and Z. Guo, *Chem. Commun.*, 2013, **49**, 2768.
17. S. V. Zutphen and J. Reedijk, *Coord. Chem. Rev.*, 2005, **249**, 2845.
18. V. Pichler; J. Mayr; P. Heffeter; O. Domotor; E. A. Enyedy; G. Hermann; D. Groza; G. Kollensperger; M. Galanksi; W.Berger； B. K. keppler and C. R. Kowol, *Chem. Commun.*, 2013, **49**, 2249.
19. H. Xiao; L. Yan; Y. Zhang; R. Qi; W. Li; R. Wang; S. Liu; Y. Huang; Y. Li and X. Jing, *Chem. Commun.*, 2012, **48**, 10730.
20. Y. Yuan; Y. Chen; B. Z. Tang and B. Liu, *Chem. Commun.*, 2014, **50**, 3868.
21. Y. Dai; X. Kang; D. Yang; X. Li; X. Zhang; C. Li; Z. Hou; Z. Cheng; P. Ma and J. Lin, *Adv. Healthcare Mater.* 2013, **2**, 562.
22. S. Dhar, Z. Liu, J. Thomale, H. Dai and S. J. Lippard, *J. Am. Chem. Soc*., 2008, **130**, 11467.
23. R. P. Feazell, N. N. Rtchford, H. Dai and S. J. Lippard, *J. Am. Chem. Soc*., 2007, **129**, 8438.
24. S. Dhar, W. L. Daniel, D. A. Giljohann, C. A. Mirkin and S. J. Lippard, *J. Am. Chem. Soc*., 2009, **131**, 14652.
25. S. N. Baker and G. A. Baker, *Angew. Chem. Int. Ed.* 2010, **49**, 6726.
26. H. Li, Z. Kang; Y. Liu and S.-T. Lee, *J. Mater. Chem.*, 2012, **22**, 24230.
27. J. C. G. E. da Silva and H. M. R. Goncalves, *Trends Anal. Chem.,* 2011, **30**, 1327.
28. C. Ding; A. Zhu and Y. Tian, *Acc. Chem. Res.*, 2014, **47**, 20.
29. M. Zheng; S. Liu; J. Li; D. Qu; H. Zhao; X. Guan; X. Hu; Z. Xie; X. Jing and Z. Sun, *Adv. Mater.*, 2014, **26**, 3554.
30. J. Tang; B. Kong; H. Wu; M. Xu; Y. Wang; Y. Wang; D. Zhao and G. Zheng, *Adv. Mater.*, 2013, **25**, 6569.
31. S. Karthik, B. Saha, S. K. Ghosh and N. D. P. Singh, *Chem. Commun*., 2013, **49**, 10471.
32. Low, P. S.; Henne, W. A.; Doorneweerd, D. D. *Acc. Chem. Res.* **2008**, *41*, 120.
33. H. Liu; T. Ye and C. Mao, *Angew. Chem. Int. Ed.*, 2007, **46**, 6473.
34. S. Choi; C. Filotto; M. Bisanzo; S. Delaney; D. Lagasee; J. L. Whitworth; A. Jusko; C. Li; N. A. Wood; J. Willingham; A. Schwenker and K. Spaulding, *Inorg. Chem.* 1998, **37**, 2500.
35. X. Wang; L. Cao; F. Lu; M. J. Meziani; H. Li; G. Qi; B. Zhou; B. A. Harruff; F. Kermarrec and Y.-P. Sun, *Chem. Commun*., 2009, 3774.
36. J. Xu; S. Sahu; L. Cao; C. E. Bunker; G. Peng; Y. Liu; K. A. S. Fernando; P. Wang; E. A. Guliants; M. J. Meziani; H. Qian and Y.-P. Sun, *Langmuir*, 2012, **28**, 16141.
37. H. Chen; R. Ahn; J. V. den Bossche; D. H. Thompson and T. V. O'Halloran, *Mol. Cancer Ther.* 2009, **8**, 1955.
38. The *trans*-Pt^{IV} azide, *trans,trans,cis*- $Pt^{IV}(N_3)_2(OH)_2(NH_3)(3\text{-}NH_2Py)$, was also covalently loaded on CDs, and the photo cytotoxicity of the relating *trans*-Pt^{IV} -N_3-FA@CDs platform (IC_{50}: ~2.0 μg_{Pt}/mL) was lower than that of the *cis*-Pt^{IV}-N_3-FA@CDs (IC_{50}: ~1.0 μg_{Pt}/mL) counterpart under similar experimental conditions.

